ADVANCED MATERIALS
www.advmat.de

The Interaction of Amines with Gold Nanoparticles

Yanchao Lyu, Lucia Morillas Becerril, Mirko Vanzan, Stefano Corni, Mattia Cattelan, Gaetano Granozzi, Marco Frasconi, Piu Rajak, Pritam Banerjee, Regina Ciancio, Fabrizio Mancin, and Paolo Scrimin**

Understanding the interactions between amines and the surface of gold nanoparticles is important because of their role in the stabilization of the nanosystems, in the formation of the protein corona, and in the preparation of semisynthetic nanozymes. By using fluorescence spectroscopy, electrochemistry, X-ray photoelectron spectroscopy, high-resolution transmission electron microscopy, and molecular simulation, a detailed picture of these interactions is obtained. Herein, it is shown that amines interact with surface Au(0) atoms of the nanoparticles with their lone electron pair with a strength linearly correlating with their basicity corrected for steric hindrance. The kinetics of binding depends on the position of the gold atoms (flat surfaces or edges) while the mode of binding involves a single Au(0) with nitrogen sitting on top of it. A small fraction of surface Au(I) atoms, still present, is reduced by the amines yielding a much stronger Au(0)–RN.$^+$ (RN$^\cdot$, after the loss of a proton) interaction. In this case, the mode of binding involves two Au(0) atoms with a bridging nitrogen placed between them. Stable Au nanoparticles, as those required for robust semisynthetic nanozymes preparation, are better obtained when the protein is involved (at least in part) in the reduction of the gold ions.

1. Introduction

Clusters of gold atoms of nanometer size (gold nanoparticles, AuNPs) are at the center of continuous and growing interest for their properties leading to numerous applications like catalysis,[1–8] sensing,[9–11] and nanomedicine.[12–14] They interact with donor atoms with different strength. These interactions are critical for the formation of a passivating monolayer on the surface of the cluster that ensures higher stability to it,[15,16] preventing nanoparticles' growth leading to flocculation with the formation of insoluble material. With reference to functional groups present in biological molecules, the strongest interaction of the gold surface of AuNPs is that with thiols, followed by that with amines and, eventually, carboxylates. The Au–S interaction has been thoroughly studied and the different aspects of it are fairly well understood.[17,18] Recent studies have also examined the nature and mode of binding of carboxylates to AuNPs.[19–21] Studies aimed at understanding the nature of the Au–N interaction have not yet provided a clear and comprehensive picture of it. Amines have been used as a weak stabilizer of AuNPs for their synthesis[22–27] and for transferring them from organic to aqueous solvents.[28,29] According to an atomistic simulation study, analyzing the effect of ligand molecules on the morphology of the nanoparticles, contrary to the Au–S interaction, the much weaker Au–N one does not perturb the crystalline structure even of very small AuNPs.[30] This weak interaction leads also to a lower degree of passivation compared with thiols.[30] Other calculations,[31–34] in the gas phase, suggest the binding to flat surfaces or edges of the nanocrystals favor the latter by ca. 4–5 kcal mole^{-1}, although the question appears to be still debated. It appears that the understanding of AuNPs' interaction with amines presents even now relevant gaps. This is particularly surprising in view of the importance of the amino functional group in biologically relevant molecules, like proteins, for instance. The interaction of amines with gold nanoparticles is probably one of the relevant driving forces leading to the formation of the protein corona when AuNPs are exposed to biological fluids for biomedical applications.[35,36] Notably, amine-stabilized AuNPs may be used to elicit further interaction with proteins for specific purposes, like targeted delivery for instance, and the preparation of nanozymes.[37–40] With this paper, we provide answers to

Y. Lyu[+], L. M. Becerril, M. Vanzan, S. Corni, M. Cattelan, G. Granozzi, M. Frasconi, F. Mancin, P. Scrimin
Department of Chemical Sciences
University of Padova
Via Marzolo, 1, Padova 35131, Italy
E-mail: fabrizio.mancin@unipd.it; paolo.scrimin@unipd.it
P. Rajak, P. Banerjee, R. Ciancio
CNR-IOM TASC Laboratory
Area Science Park
Basovizza S.S. 14, km 163.5, Trieste 34149, Italy
P. Rajak, P. Banerjee
Abdus Salam International Centre for Theoretical Physics
Via Beirut, 6, Trieste 34151, Italy
R. Ciancio
Area Science Park
Padriciano 99, Trieste 34149, Italy

The ORCID identification number(s) for the author(s) of this article can be found under https://doi.org/10.1002/adma.202211624

[+]Present address: School of Chemistry and Chemical Engineering, Yangzhou University, Yangzhou, Jiangsu 225002, China

DOI: 10.1002/adma.202211624

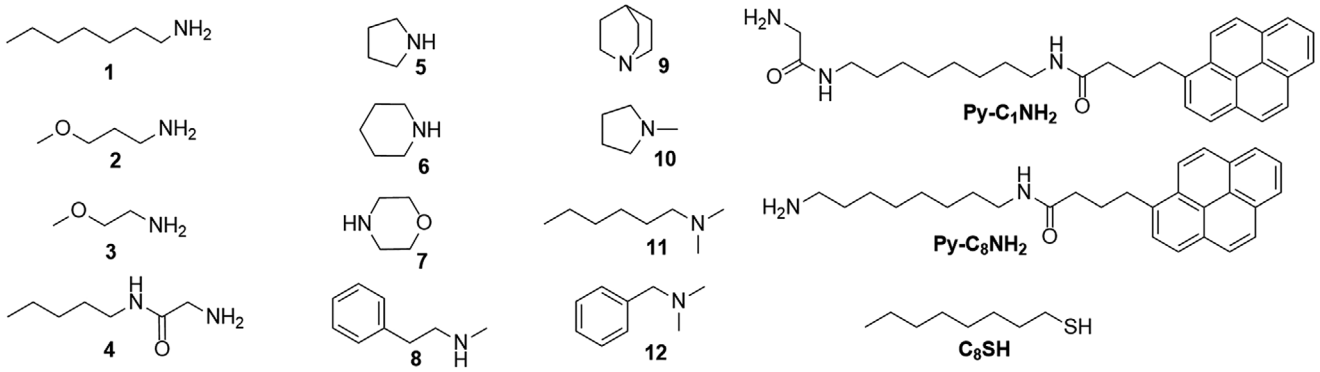

Figure 1. Amines used in this study (1–4, primary, 5–8, secondary, 9–12, tertiary) and thiol employed for the total removal of the fluorescent amine (right) from the AuNPs surface.

questions concerning the nature of the interaction of amines with the AuNP surface by addressing their mode of binding to the surface and how the properties of an amine (like basicity, the level of substitution on the nitrogen) and the oxidation state of the surface Au atoms affect the strength and kinetics of this interaction.

2. Results and Discussion

2.1. Gold Nanoparticles and Amines Studied

Since most of the gold nanoparticles, particularly those used for biological applications, are prepared following the Turkevich protocol,[41] we have chosen this procedure for their preparation. This implies that no other reducing agent (like $NaBH_4$, for instance) but sodium citrate was used for their synthesis. Furthermore, for analytical applications, they must be endowed with optical properties related to a strong surface plasmon resonance (SPR) band. This is present only when the AuNPs have a diameter $>\approx$3 nm and increases in intensity with the nanoparticle size. For this reason, we have chosen as our reference model, AuNPs with a diameter of ≈10 nm (see Figures S1 and S2, Supporting Information). They can be obtained with ease and reproducibility[41,42] than bigger ones by reduction with sodium citrate, using the Ag seeding protocol. To assess the nature and the strength of the interaction of amines with the AuNPs surface we removed most of the citrate (and oxidized products formed) present. In spite of their weak interaction with the gold surface, it has been reported that citrate ions may interfere with the binding of other passivating molecules (even thiols).[43] Four washings/centrifugation cycles performed after their preparation resulted in a substantial, but not total, removal of the citrate, as expected.

Thermogravimetric analyses performed before and after the washings indicated that the organic component was reduced to ≈25% of the original one (see Figure S3, Supporting Information). The Z-potential of the as-prepared AuNPs was −25.5 mV while that of the "citrate-depleted" was much less negative (−2.5 mV). Our calculations indicate that still the concentration of citrate is ≈34% of the gold atoms present on the surface (see the Supporting Information). This was the minimum amount of citrate ions that allowed us to obtain stable solutions without aggregation of the nanoparticles as evidenced by the absence of changes in the SPR band (position and intensity) for the time course of our experiments. We will refer to these AuNPs as "naked" ones.

We have selected amines spanning a wide range of basicity comprising primary, secondary, and tertiary ones (**Figure 1**). Since several of these amines, as neutral, non-protonated species were sparingly soluble in water, we have chosen ethanol as our solvent. Ethanol affects the absolute basicity of amines. However, although its effect is different for primary, secondary, and tertiary ones, within each class the relative basicity is not altered, and appropriate correction coefficients are available to normalize this property between them.[44] Extreme care should be used in studying "naked" AuNPs in a non-aqueous solvent such as ethanol because even small amounts of salt are known to induce their aggregation.[45] This is related to the formation of oppositely charged particles in a less solvating medium than water.[46]

2.2. The Basicity of the Amines Controls Their Interaction with the Gold Surface

To assess what controls the strength of the interaction of the different amines with the surface of the AuNPs we carried out exchange experiments with a fluorescently labeled amine (Py-C_1NH_2, Figure 1) used to fully passivate the gold nanoparticles. The experiment takes advantage of the well-known quenching of fluorescent molecules when bound to a gold nanoparticle surface.[47,48] Accordingly, "naked" AuNPs were dissolved in ethanol and the fluorescence of the solution was monitored following the progressive addition of Py-C_1NH_2. The obtained profile (**Figure 2**A) reveals the concentration at which the surface is fully saturated by the amine (surface saturation concentration, SSC) as the break point between the flat portion of the curve (fluorescence is quenched) and the steep straight line (fluorescence no longer quenched).[49] The obtained SSC is 1.64 μM (for a 8.6 nM AuNPs[50] concentration, see the Supporting Information). For our 9.7 ± 1.3 nm AuNPs this implies a surface density of slightly less than one Py-C_1NH_2 molecule nm^{-2}.[42] It has been estimated that thiols passivation leads to surface densities ranging from 7 to 3 ligands nm^{-2} depending on the structure of the thiol.[42,51] In our case, the lower density could be related to the bulkiness of the pyrene moiety, the fact that the footprint of an amine (not deprotonated, contrary to a thiol) is bigger, or its weaker

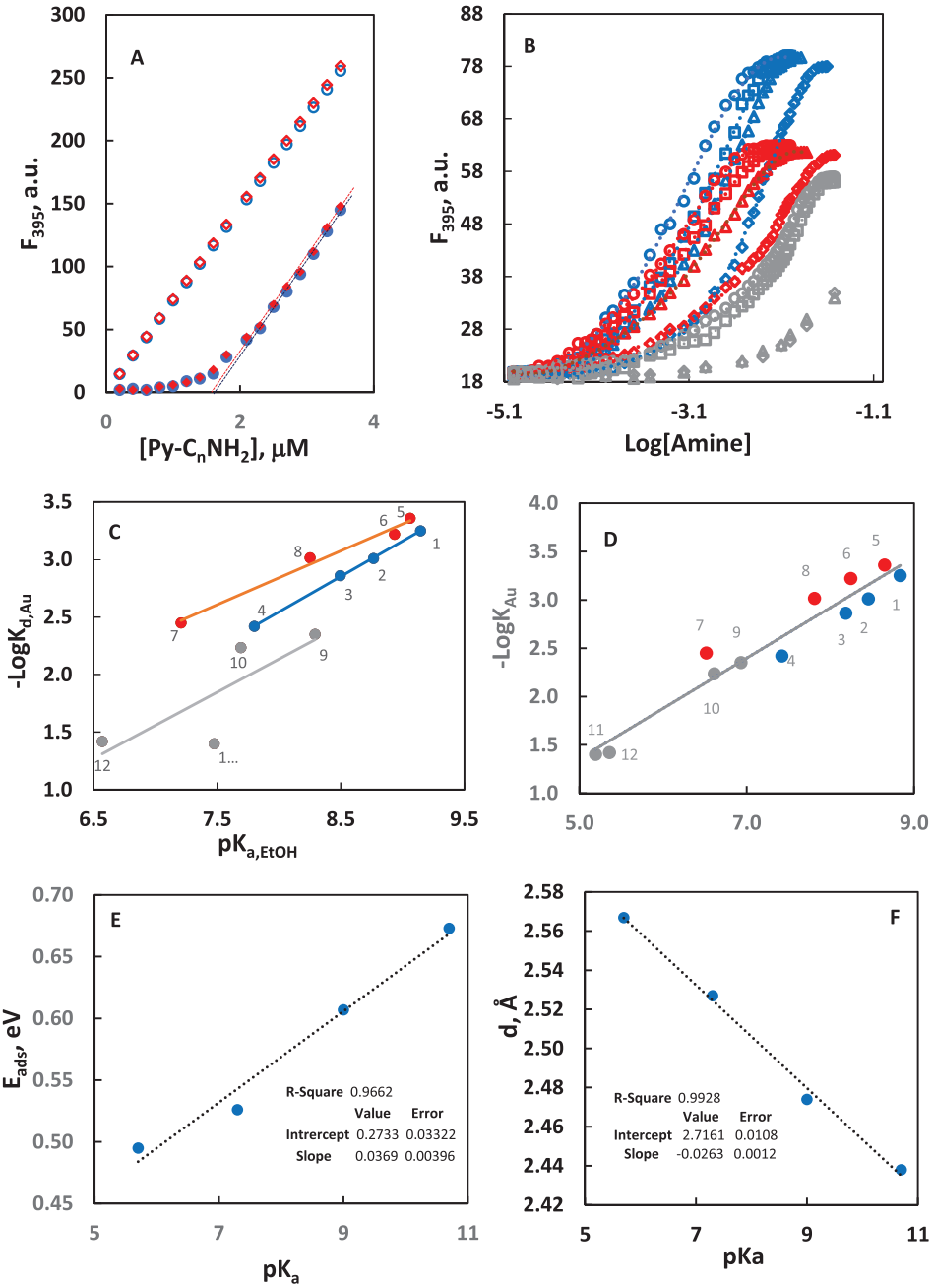

Figure 2. A) Fluorescence intensity (395 nm) as a function of the concentration of added amines Py-C_1NH_2 (red diamonds) and Py-C_8NH_2 (blue circles) to ethanol (empty symbols) and to a solution of nanoparticles (filled symbols). The intersection between the two straight lines was taken as the surface saturation concentration (SSC). Conditions: 35 °C, EtOH, [AuNPs] = 8.6 nM. B) Binding isotherms obtained by following the F_{395} upon addition of increasing amounts of amines **1**–**12**. In blue: primary amines, red, secondary, gray, tertiary. Circles: amines **1**, **5**, **9**; squares: amines **2**, **6**, **10**; triangles: amines **3**, **8**, **12**; diamonds: amines **4**, **7**, **11**. Conditions as for panel (A). C) Log plot of the pKa in ethanol of the amines and their apparent dissociation constant for the gold surface obtained by interpolation of the data of (B). Data were fitted by linear regression analysis. For amines **11** and **12** F_{max} was arbitrarily set at the value of that obtained for amine **9**. Errors for affinity constants (two independent measurements) are ±5% for amines **1**, **2**, **5**, **6**, **8**; ±7% for amines **3**, **4**, **7**, **9**, **10**; and ±15% for amines **11** and **12**. D) Log plot of the pKa in ethanol of the amines corrected for the steric hindrance parameter Es (see Table 1) and their apparent dissociation constant for the gold surface obtained by interpolation of the data of (B). Data were fitted by linear regression analysis. All other conditions were identical to those of (C). E) Adsorption energies (E_{ads}) calculated for amines $NH_2CH_2CH_3$, $NH_2CH_2CH_2F$, $NH_2CH_2CHF_2$, $NH_2CH_2CF_3$ on Au(111) surfaces plotted against their pKa. F) Measure of the N–Au distance (d) for the four amines from the Au atom of the (111) surface as a function of their pKa. For both panels (D) and (E), the red lines were obtained through a linear regression fit of the data; fitting parameters are contained within the inset tables of each panel.

Table 1. Relative dissociation constants for the AuNPs surface of amines **1**–**12**, their reported pK_a in EtOH and steric hindrance parameters (Es) used for the analysis of the data.

Amine	$pK_{a,\ EtOH}$ [a]	$pK_{d,Au}$ [b]	−Es[c]	Amine	$pK_{a,\ EtOH}$ [a]	$pK_{d,Au}$ [b]	−Es[c]
1	9.15	3.25	0.31	**7**	7.21	2.45	0.69
2	8.77	3.01	0.31	**8**	8.25	3.01	0.44
3	8.50	2.86	0.33*	**9**	8.29	2.35	1.36*
4	7.80	2.42	0.35*	**10**	7.69	2.23	1.08*
5	9.06	3.36	0.41	**11**	7.48	1.40	2.28
6	8.94	3.22	0.69	**12**	6.57	1.42	1.21

[a] Values were obtained from the pKa in water and converted by using the equations reported in ref. [44]; [b] Errors are indicated in the caption to Figure 2C; [c] Values obtained from refs. [58] and [59]; those indicated by an asterisk were extrapolated (see ref. [59]).

interaction with respect to a thiol with the gold nanoparticle surface.[29,52]

By using AuNPs passivated at the $[Py\text{-}C_1NH_2]_{SSC}$ we then performed exchange experiments with amines **1**–**12** (Figure 1) monitoring the increase of fluorescence due to the release of $Py\text{-}C_1NH_2$ from the AuNPs surface and obtained the binding isotherms shown in Figure 2B (see also Figure S4, Supporting Information). The obtainment of the final equilibrium requires a few hours at 35 °C and a concentration $> 6 \times 10^{-3}$ M of entering amine for the most basic ones for achieving the maximum attainable exchange. For the least basic ones, on the contrary, a 3×10^{-2} M concentration, the maximum possible without observing aggregation of the nanoparticles, was not enough to reach the total exchange and only ≈50% of it was observed. We were really surprised by this difference in concentration between exiting (1.64 μM) and entering ($>6 \times 10^{-3}$ M) amine. However, considering that the fluorescent amine $Py\text{-}C_1NH_2$ is confined in the monolayer passivating the gold nanocluster core with an estimated thickness of ≈3 nm (the estimated length of the fully extended $Py\text{-}C_1NH_2$ probe), its actual concentration in this restricted space surrounding the gold core is $\approx 4 \times 10^{-2}$ M (see the Supporting Information for details). This implies that strong π–π stacking interactions do occur between the pyrene units as it has already been observed.[53] Reported molecular calculations indicate that they do not interact with the surface of the AuNPs.[54] These interactions add up to the binding driven by the interaction of the amine with the gold surface greatly enhancing the overall affinity of $Py\text{-}C_1NH_2$ for the AuNPs. The π–π stacking of several pyrenes confined on the small volume of the monolayer can easily increase the affinity of $Py\text{-}C_1NH_2$ by approximately three orders of magnitude to make up for the concentration of entering amine required for its full displacement.[55] Interestingly, when passivating the AuNPs surface with $Py\text{-}C_8NH_2$ (SSC = 1.62 μM) we were unable to observe more than 20% exchange at the highest concentrations of entering amine used (data not shown). It should be pointed out that the pyrene units on one side contribute to a stronger affinity but on the other, because of steric hindrance decrease the density of passivation of the surface.[42]

Interpolation of these curves provided the apparent, relative dissociation constants of the different amines for the AuNPs surface ($pK_{d,Au}$ **Table 1**). By plotting the $pK_{d,Au}$ values versus the pK_a of the amines, corrected for ethanol as the solvent ($pK_{a,EtOH}$),[44] we obtained the graph reported in Figure 2C. The existing correlation between the $pK_{a,EtOH}$ of the amines and the strength of their interaction with the nanoparticle surface indicates there is a linear free energy relationship (LFER) between the proton affinity constant and that for the gold surface. This correlation is very good for primary and secondary amines ($r^2 = 0.996$ and 0.984, respectively) but poor for tertiary ones ($r^2 = 0.646$). Steric effects are very likely at play for two reasons. First, each class of amines belongs to a different straight line. Second, tertiary amines' points are rather scattered. In order to take into account steric hindrance, Taft introduced experimental parameters (Es) derived from the kinetic analysis of the hydrolysis of esters with aliphatic substituents. These parameters have been updated over the years and theoretically validated for their physico–chemical significance.[56,57] We have used an extended database by Dubois[58] that provides also hints for the estimate of missing data.[59] For the correlation, we have applied the equation $pK_{d,Au} = \text{cost}\ (pK_{a,EtOH} + Es)$. The Es parameters we have used are listed in Table 1. The resulting plot is shown in Figure 2D. Very interestingly, all points could be fitted with a single straight line with a fairly good correlation coefficient ($r^2 = 0.941$), even though small differences between the three classes of amines are still present. Notably, the scatter of the points for the tertiary amines disappeared almost completely. The relevance of steric factors in the binding of the amines to the gold nanoparticle suggests that the exposure of the nitrogen to the surface affects the strength of the interaction.

LFERs were first introduced to quantitatively correlate reactivity with structural parameters of organic molecules. They have been extended to the complexation of metal ions by Irving and Rossotti[60] and have been applied to stability constants for metal ligands complexes, including those containing neutral nitrogen donor atoms.[61] Conceptually, the graphs of Figures 2C,D are not much different from a Brønsted plot used in nucleophilic reactions.

Accordingly, the slope of the straight lines would indicate how much the affinity of the amines for the proton is reflected in its affinity for the gold surface. The slopes for the three straight lines of Figure 2C are 0.62, 0.47, and 0.58 for primary, secondary, and tertiary amines, respectively, while that of Figure 2D is 0.52. From these data, we infer that, while basicity and affinity for the gold nanoparticle surface do in fact correlate, the lone pair electrons of the amines are better shared with a proton than with a gold atom on the AuNP surface. A similar slope (0.48) was observed by Carbonaro in the case of complex formation of amines with Cu(II) ions.[61] The dependence of the strength of binding from the $pK_{a,EtOH}$ also provides an explanation why $Py\text{-}C_1NH_2$ can be fully displaced by the entering amines while $Py\text{-}C_8NH_2$ much less: the $pK_{a,EtOH}$ of the first dye should be slightly less than two units lower than that of the second one (as they are expected to be similar to those of amine **4**, $pK_{a,EtOH} = 7.8$ and **1**, $pK_{a,EtOH} = 9.1$, respectively, see Figure 1). Accordingly, the contribution to binding of $Py\text{-}C_8NH_2$ due to the Au–N (lone pair) interaction is at least one order of magnitude larger than that of $Py\text{-}C_1NH_2$. It is also worthwhile noting that the addition of H_2O (up to 20%) to the ethanol solution results in a decrease in the apparent affinity constant of amine **1** to the gold nanoparticles (Figure S5, Supporting Information). Water is hence a more competitive solvent

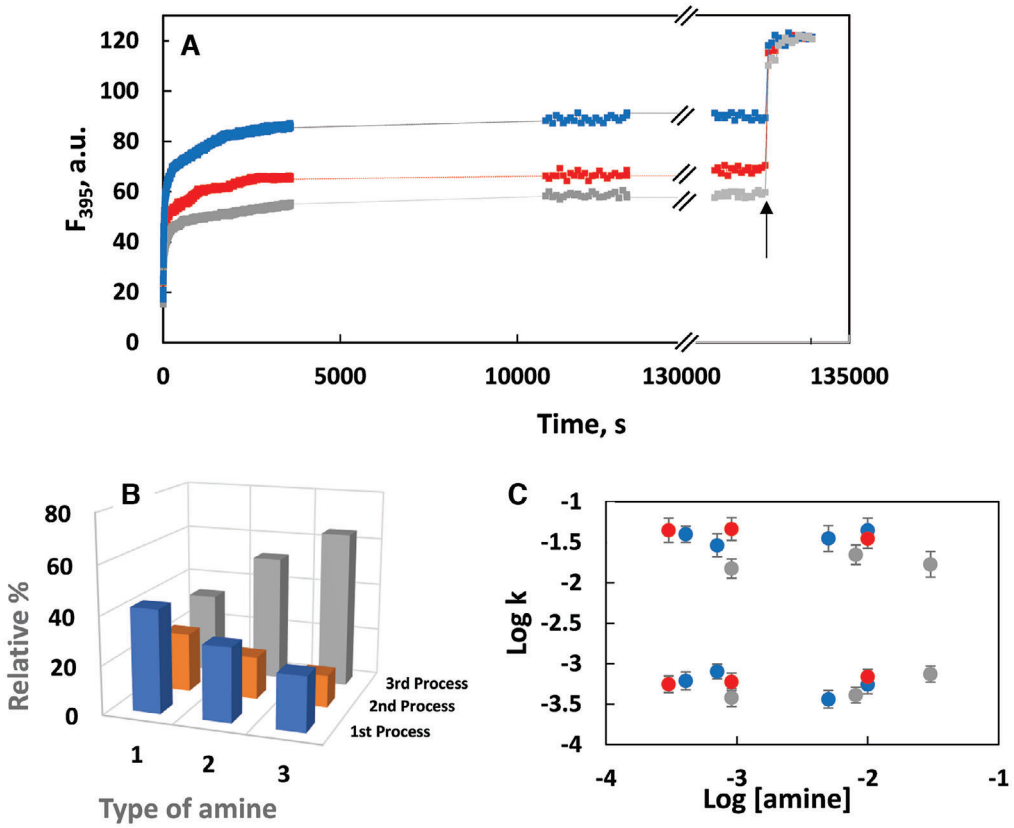

Figure 3. A) Increase of fluorescence (at 395 nm) as a function of time upon addition of amines **1** (blue), **5** (red) and **9** (gray) to [AuNPs] = 8.6 nM passivated with $[Py\text{-}C_1NH_2]_{SSC}$ in ethanol at 35 °C; [1] = [5] = 7.1×10^{-4} M; [9] = 9.1×10^{-4} M. Data were fitted with a double exponential equation. Note the difference in time scale in the right part of the graph. The arrow indicates the addition of thiol C_8SH. Note that by following the kinetics for a longer time (up to 72 h) no change in fluorescence was observed. B) Relative percentage of the three kinetic processes represented in (A) (1, 2, and 3 are the primary, secondary, and tertiary amine, respectively). C) Dependence of the rate of exchange of amine $Py\text{-}C_1NH_2$ from the entering amines **1**, **5**, and **9** concentrations (blue, red, and gray symbols, respectively) at 35 °C in ethanol.

than ethanol for the surface of the AuNPs. It is well known that the nature of the solvent affects nucleophilic substitutions.[62] In this regard, ethanol and water are significantly different solvents.

The relevant role of the basicity of the amines in affecting their interaction with the gold surface was confirmed by density functional theory (DFT) calculations performed on systems composed by a Au(111) planar surface interacting with amines $NH_2CH_2CH_3$, $NH_2CH_2CH_2F$, $NH_2CH_2CHF_2$, $NH_2CH_2CF_3$, with pK_a (in water) 10.7, 9.0, 7.3, 5.7, respectively.[63] Figure 2D shows there is a linear relationship between their pK_a and the energy of adsorption to the gold surface, calculated according to Equation (1) (see Computational Methods section in the Supporting Information). Remarkably, translating the adsorption energy differences directly into differences of $-\log K_{Au}$, the expected slope of the $-\log K_{Au}$ versus pKa correlation is around 0.6–0.7, in line with the experimental finding for primary amines (0.62 as reported here above, without considering steric effects). This further supports that the Au–N binding strength, in turn related to the basicity of the amines, is the key determinant of the observed effect. Furthermore, the more basic the amine is, the shorter is the Au–N distance, again following a linear relationship with their pK_a (Figure 2E).

2.3. The Exchange Process on the AuNP Surface is Multimodal

The above affinity constants were determined at the very end of the exchange process that requires a few hours to reach the final equilibrium at 35 °C. However, by examining in detail the kinetics of this exchange we observed two important things. First, the time dependence of the release of the fluorescent dye from the gold surface follows a bimodal kinetic with a fast process followed by a much slower one. Second, the removal of the fluorescent amine $Py\text{-}C_1NH_2$ is never total, and the 100% fluorescence increase is only obtained by addition of a thiol (C_8SH, Figure 1) to the solution. A typical kinetic profile is reported in **Figure 3**A. The kinetics have been performed with three representative amines, chosen for their strongest apparent affinity constant for the gold surface for each category: *n*-heptylamine, **1**, as a primary amine; pyrrolidine, **5**, as a secondary amine; quinuclidine, **9**, as a tertiary amine. **Table 2** reports the rate determined for the first two exchange processes and the relative percentage of each of them. The percentage of the last process for which the addition of a thiol is necessary in order to totally remove $Py\text{-}C_1NH_2$ from the surface is also reported. Figure 3B reports these percentages in graphical form.

Table 2. Kinetic parameters for the exchange of amine Py-C_1NH_2 from the surface of AuNPs with entering amines **1**, **5**, **9**. Conditions: 35 °C, EtOH, [**1**] = [**5**] = 7.1×10^{-4} M; [**9**] = 9.1×10^{-4} M.

Amine	10^2 k_{fast} [a]	% k_{fast}	10^4 k_{slow}	% k_{slow} [b]	% not exchanged[c]
1	2.9	42	8.0	24	34
1[d]	2.0	61	6.0	36	3
5	4.6	31	9.1	18	51
9	1.5	22	3.8	13	65

[a] Kinetics were run in triplicate; error ±10% [b] Kinetics were run in triplicate; error ±6% [c] Based on the final fluorescence observed after the addition of thiol C_8SH [d] Using AuNPs treated with $NaBH_4$.

For the three amines the first exchange process is ≈40-fold faster than the second one without a significant difference between primary, secondary, and tertiary ones. The overall percentage of exchanged amine in the course of the first two kinetic processes decreases from 67%, to 48%, and 36% for the primary, secondary, and tertiary amine, respectively, suggesting that steric hindrance plays a role also in determining the number of exchangeable amines by the entering ones. Nitrogens with a larger number of substituents have a larger footprint on the nanoparticle surface and, accordingly, a lower number of them can be accommodated on each AuNP. Upon addition of thiol C_8SH the final fluorescence observed is the same in all cases, implying that all amines attached to the AuNPs are replaced by thiols regardless of their mode of interaction with the gold surface. However, the relative percentage of the first, faster process with respect to the second, slower one is 63:37 for all amines studied. This observation suggests that there are two types of exchangeable Py-C_1NH_2 bound to the AuNP, indicating the presence of different gold atoms on the nanoparticle surface. A third type can only be exchanged by using a thiol, as said above and as will be discussed below.

Possible explanations for this behavior could refer to the type of gold atoms to which the amine is bound, or the type of crystal formed during the synthesis of the nanoparticle. A similar bimodal kinetic exchange behavior has been observed for thiols.[66,67]

To assess the type of crystals formed in the nanoparticle preparation, their structural properties were investigated by TEM. **Figures 4**A,E show the bright-field microscopy images of "naked" and Py-C_1NH_2-passivated AuNPs, respectively. AuNPs in both samples have a comparable spherical shape in order to minimize the surface energy. The difference in particle size (see also Figures S1 and S2, Supporting Information) between the "naked" AuNPs (9.3 ± 1.5 nm) and the amine passivated ones (9.7 ± 1.3 nm) is not particularly relevant. High-resolution TEM (HRTEM) imaging gives further insight into the ultrastructure of the AuNPs. The HRTEM images show that both samples consist of AuNPs with icosahedral, decahedral, and cuboctahedral shapes. The corresponding atomistic models of icosahedral, decahedral, and cuboctahedral shapes are included as figure insets for ease of visualization. These types of particles are very frequent in the AuNPs. Figures 4B–D, and 4F–H allow one to appreciate the fringe spacing of 0.28 nm of spherical gold nanoparticles. In accord with what reported by Mariscal et al.,[30] the structure of the nanoparticles is not affected by the passivation with the amine (compare, in Figure 4B–D with Figure 4F–H), contrary to what happens with thiols.[30] Notably, the relative percentage of the three shapes is very similar and does not change after passivation (Figure S6, Supporting Information).

This trimodal crystal distribution characterized by very similar relative fractions seems to exclude the hypothesis that the kinetic dependence of the exchange process is related to the type of crystal to which the amine is bound. A more likely reason relies on the sort of gold atom to which the amine is attached, those on flat surfaces or those on rims and vertexes. Flat surfaces, rims, and vertexes are common features of all three types of crystals present in our gold nanoparticles preparations. Reported calculations reveal that the ratio between gold atoms residing on edges or flat surfaces strongly depends on the particle size for the smallest nanoparticle reaching a ≈30:70 value that remains practically

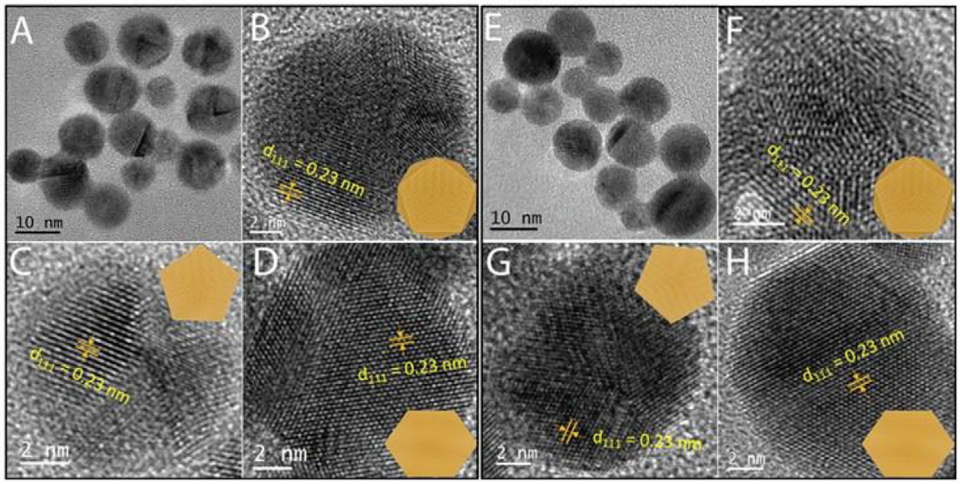

Figure 4. A,E) TEM bright-field microscopy images of the gold nanoparticles as prepared ("naked") and passivated with Py-C_1NH_2. B–D) HR-TEM images of AuNPs with icosahedral, decahedral and cuboctahedral shape of as prepared sample, respectively. F–H) HR-TEM images of NPs with icosahedral, decahedral, and cuboctahedral shape of AuNPs passivated with Py-C_1NH_2 at SSC, respectively. In the insets the atomistic models of icosahedral, decahedral, and cuboctahedral shapes are presented.

constant as the size further increases (up to ≈4.5 nm in diameter, the largest size reported).[64] Although this ratio depends on the crystal structure, too, the difference is within ±10% for gold nanoparticles. It is tempting to cautionary extrapolate these values for our larger 10 nm nanoparticles as the numbers are rather close to the 37:63 ratio between the slow and fast processes we observe. In the case of amines, computational analysis has indicated as the strongest interaction that occurring with atoms at edges and vertexes.[33] Furthermore, for catalytic application it has been shown that gold atoms with lower coordination number (≤6), like those on edges and rims, generally manifest lower adsorption energies and hence a stronger binding of the substrate.[65]

Very important is the observation that the kinetics of both exchange processes for the three types of amines studied (primary, secondary, and tertiary) do not depend on the concentration of the incoming amine (Figure 3C). This indicates a dissociative (S_N1-like) reaction mechanism in which the displacement of the amine is not the rate determining step. The great majority of the studies of the kinetics of the exchange of thiols bound to AuNPs support an associative mechanism (S_N2-like).[66–69] This difference might be related to the strength of the interaction between the ligand and the gold surface with a switch from associative to dissociative mechanism with more weakly bound ligands, like amines. Interestingly, a dissociative mechanism has been reported for the exchange of weakly-bound cetyltrimethylammonium bromide with entering thiolated ligands.[70] A dissociative mechanism would support a thermodynamic dependence of the exchange process. With a dissociative mechanism, the more weakly-bound amine would be detached first even if it is less accessible to the incoming one. This is the case of those residing on flat surfaces (more packed, less accessible) with respect to those on edges (less packed, more accessible). On the contrary, an associative mechanism would lead to the opposite behavior as it has been suggested for thiols. In that case, thiols bound to edges, vertexes, or defects of the surface of the nanoparticle exchange faster than those bound to flat surfaces.[67] Although not conclusive, the existing computational data[33] on the stronger binding to edges than to flat surfaces and the present kinetic results strongly support the suggestion that amines residing on flat surfaces, that is, (111) or (100), exchange faster than those on edges.

2.4. A Redox Process is Likely Involved in the Most Tightly Bound Fraction of Amines

We were really intrigued by the failure of all entering amines to fully exchange all Py-C_1NH_2 bound to the AuNPs surface. We have followed the exchange with the entering amine up to the thermodynamic equilibrium. Thus, no kinetic issues appear to be present. We infer that the non-exchangeable fraction of Py-C_1NH_2 should have a significantly higher affinity (at least two orders of magnitude) than the amine-exchangeable one since it can only be displaced from the gold surface by using a thiol. It seems very unlikely that this binding process occurs by involving the lone electron pair on the amine as in the case of the amine-exchangeable fraction. Our "naked" AuNPs, prepared by using a mild reducing agent as sodium citrate, contain a significant fraction of surface Au(I) (≈9% as estimated by XPS data, **Figure 5**A).[19] The presence of oxidized gold should not be surprising since its redox potential (E_o(Au(I)/(Au(0)$_{aq}$) becomes negative when hydrated Au(0) clusters are formed.[71,72] We hypothesized that these Au(I) atoms could oxidize the amino group yielding a radical cation (Py-$C_1NH_2^{+\cdot}$).[73] Such radical cations have been reported to lose a proton relatively fast to yield a strong Au(0)–RN bond.[74] The occurrence of such a redox process is supported by the disappearance of surface Au(I) atoms in the XPS spectrum after passivation with heptylamine (**1**) at the SSC (Figure 5B). Amine **1** was selected for the presence of a single nitrogen atom contrary to Py-C_1NH_2 and its SSC, as a primary amine, was assumed to be very similar to that of the fluorescent amine. The corresponding N 1s XPS region of the passivated AuNPs is reported in Figure 5C: although very noisy for the very little concentration of amine present, the broad signal could be fitted considering three components with binding energy (BE) of 398.2, 399.6, and 401.0 eV (Figure 5C).

The data in the literature on the N 1s region in similar studies are rather scattered. In many cases the fitting has been done with an unrealistically large FHWM value for some component which takes to only two components.[52] We preferred to adopt a physically acceptable FHWM of 1.6 eV, leading to three different components.[74] Similarly, the assignment of the different components is rather controversial in literature, apart from the highest BE one, which is always assigned to oxidized amine.[52] To avoid any speculation on these, we prefer to assign the three components heuristically: the 399.6 eV BE component is the typical one related to **1** grafted on the gold surface, the component at 401.0 could indicate the presence of a slightly positively charged N, different from a protonated nitrogen which would be expected at a little higher BE.[44] On the other hand, the component at 398.5 eV BE could be related to slightly negatively charged nitrogen.[74,75] These results appear to indicate the coexistence of $RNH_2^{+\cdot}$ and $RNH^{\cdot}$ bound to the surface Au(0) atoms. As mentioned above, it has been reported, in contradiction to what we find here, that a radical cation of a primary amine loses a proton very quickly to give a radical.[74] In any case, whatever its protonation state is, a radical is formed that tightly binds to the gold surface. One might argue that the fraction of primary amine bound as a radical/radical cation is too high when compared with the amount of Au(I) present on the nanoparticle surface (compare with the 9% obtained from the XPS spectra). However, considering that only a fraction of the surface gold atoms interacts with the amine (≈10%, according to our calculations, see Supporting Information), the amount of Au(I) is more than enough to oxidize the amine that eventually tightly binds to the gold nanoparticle surface (as a radical/radical cation). Since this is an irreversible process, all available amines are captured by the available Au(I) ions present on the surface at the expenses of those binding through the lone electron pair interaction to reach the maximum surface coverage attainable under our experimental conditions.

The higher affinity of the radical toward the gold surface was also investigated by means of DFT calculations. Adsorption energies were sizably more favorable for the radical than for the corresponding amine with a significant change also in the adsorption morphology. As an example, considering the species that has been suggested to actually adsorb on the metal surface following the amine oxidation (i.e., $\cdot NHCH_2CH_3$ vs the standard $NH_2CH_2CH_3$ amine),[74] we estimate an adsorption energy

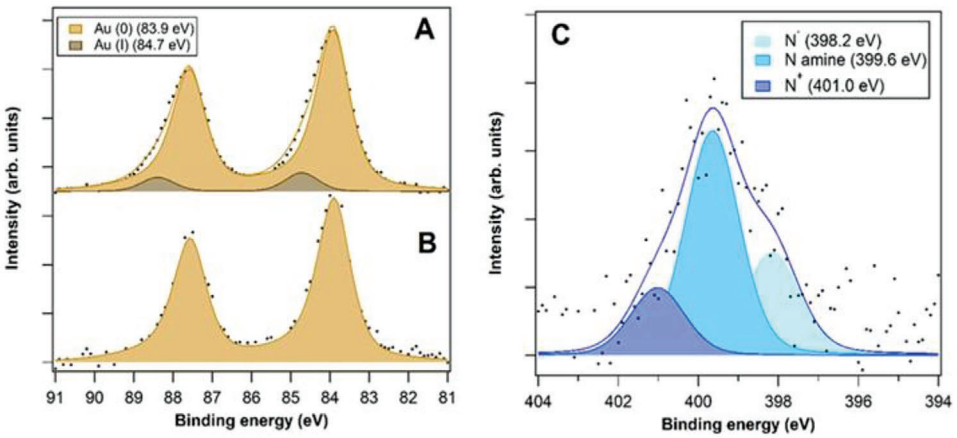

Figure 5. A,B) Au 4f core level XPS data of "naked" (A) and passivated with n-heptylamine (**1**, 1.2 μM) AuNPs (B). The data were fitted with a doublet with the Au $4f_{7/2}$ at 83.9 eV (Au(0)) and at 84.7 eV (Au(I)). C) Analysis of the N 1s photoemission line in the XPS spectrum of AuNPs passivated with 1.2 μM **1**. By setting a FWHM of 1.6 eV for each component three bands were needed to achieve a satisfying fitting.

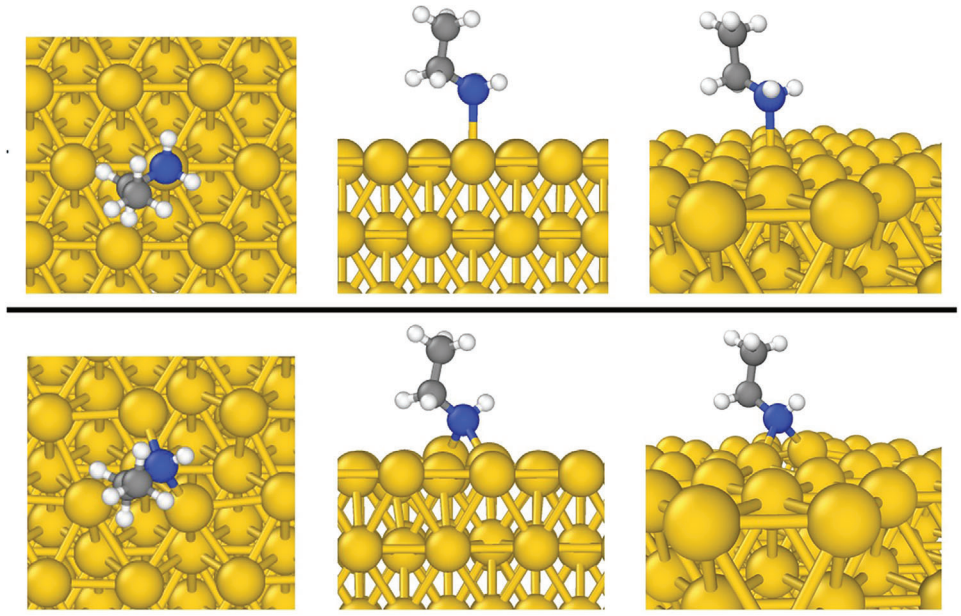

Figure 6. A,B) DFT simulation of the adsorption mode of ethyl amine on an Au(111) surface as a neutral species (A) and as an oxidized radical (B). Notice as in this latter case no adatoms formation was observed thus maintaining unaltered the crystal structure in accordance with the HRTEM images.

around −1.1 eV which is significantly more negative compared to the −0.673 eV found in the case of the standard form. The adsorption configuration is also different with reference to the neutral amine, bridging between two Au(0) atoms (**Figure 6**B) instead of being on-top (Figure 6A). All these findings are compatible with what is already known about the adsorption of amine radicals on gold surfaces.[76] Importantly, no adatoms formation was observed when the interaction of the radical with the Au(111) surface was simulated thus maintaining unaltered the crystal structure in accordance with the HRTEM images.

Following this line of reasoning we argued that the total reduction of Au(I) atoms would make all Py-C_1NH_2 molecules exchangeable by the entering amine while the independent oxidation of the amines passivating the gold nanoparticles would completely prevent their exchange. The full reduction (as indicated by XPS) was achieved by treatment with $NaBH_4$. Thus, fully reduced AuNPs were passivated with Py-C_1NH_2 at SSC and subsequently exposed to amine **1** (under identical conditions as those used for the original, partly oxidized AuNPs) and the exchange process was followed with time. The results are reported in **Figure 7**A together with those obtained for the original system, for comparison. Very interestingly, the exchange proceeded up to ≈97% (compare with the 66% observed with the original, partly oxidized AuNPs). It could be analyzed as a bimodal kinetic with a rate for the fast and slow process of 2.0×10^{-2} and 6.0×10^{-4} s^{-1}, respectively. The relative fraction (slow/fast) was 38:62. These numbers are in good agreement with those obtained with the original system.

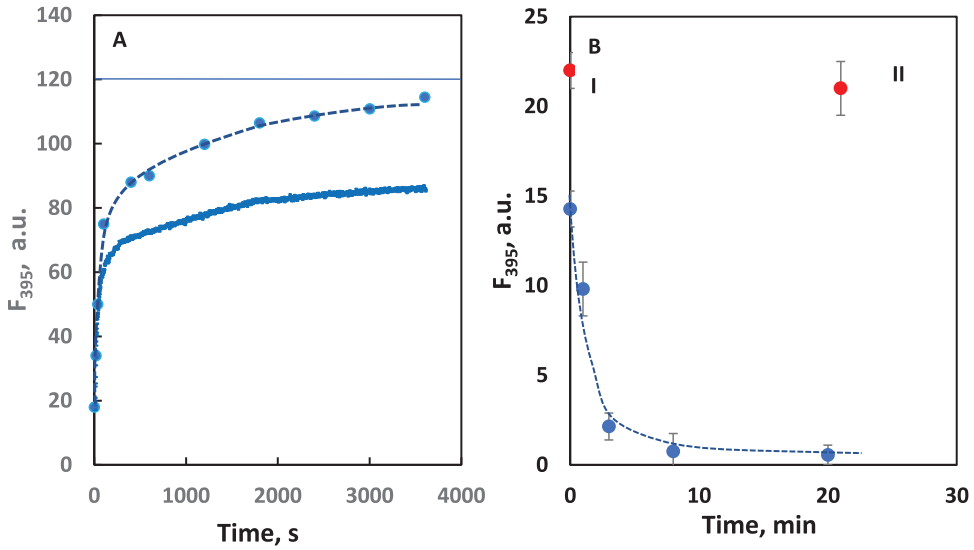

Figure 7. A) Kinetic of the exchange process between amine Py-C_1NH_2 and **1** using AuNPs treated with $NaBH_4$ (blue circles). The dashed line represents the fitting of the two kinetic processes. The horizontal line at $F_{395} = 120$ represents the maximum fluorescence obtained by addition of thiol C_8SH. For comparison, the exchange kinetics of the same amines but using AuNPs not treated with $NaBH_4$ is reported. The conditions are the same as those of Figure 3A. B) Fluorescence observed in solutions obtained after the addition of an excess of amine **1** to the GC electrode modified with the AuNPs passivated with 1.6 μM Py-C_1NH_2 following increasing oxidation times (conditions: 1.1 V vs Ag/AgCl, CH_3CN, 0.1 M $TBAPF_6$). The red points indicated with I and II represent the fluorescence measured for solutions collected at time 0 (I) and 20 min (II) upon addition of thiol C_8SH. Each point represents a different experiment. The experiments were run in duplicate. The dashed line was drawn to guide the eye.

As for the oxidation of amines passivating gold nanoparticles, to avoid side reactions on the AuNP surface by the addition of oxidizing agents in solution, the process was enacted electrochemically. Accordingly, AuNPs passivated with $[Py\text{-}C_1NH_2]_{SSC}$ were deposited on a glassy carbon electrode and the electrochemical oxidation was investigated by cyclic voltammetry in CH_3CN with 0.1 M $TBAPF_6$. The modified electrode shows an irreversible oxidation peak at about 0.94 V versus Ag/AgCl, associated with the oxidation of the amines (Figure S12, Supporting Information). A decrease in the signal intensity of this peak was observed in the second and third scan, a phenomenon that can be ascribed as consequence of an irreversible process of the oxidized amine on the AuNPs surface. To probe the effect of amine oxidation on its exchange ability, the voltage of the GC electrode modified with AuNPs passivated with $[Py\text{-}C_1NH_2]_{SSC}$ was set at 1.1 V, n-heptyl amine (**1**) was added after increasing oxidation times, and the fluorescence of the solution measured. The graph of Figure 7 shows that, as the oxidation time increases, the amount of exchangeable amine decreases with almost no increase of fluorescence after 20' of oxidation time. However, C_8SH addition was able to release the AuNP-bound Py-C_1NH_2 reaching a fluorescence comparable to that obtained by addition of the same thiol at time zero. Control experiments showed that the oxidation potential used was not affecting either gold or pyrene confirming that only the primary amine was oxidized during the electrochemical experiment. Overall, these experiments are consistent with a binding process of the fluorescent primary dye occurring not through the lone pair electrons of the amine but through the formation of a stronger Au–N bond involving a radical/radical cation.[74,77]

Thus, the passivation of the surface of AuNPs containing a fraction of Au(I) atoms leads to the formation of two populations of bound amines: those not oxidized and the oxidized ones. The not oxidized fraction easily exchanges with entering amines (**Figure 8**, first and second steps). On the contrary, the oxidized fraction only exchanges with ligands having a much stronger affinity than amines for the gold surface, as thiols do (Figure 8, last step).

3. Conclusion

The overall picture emerging from the study of the binding of amines to gold nanoparticles prepared with the classical Turkevich protocol reveals that most of them interact with the gold atoms on the surface with the lone pair electrons of the nitrogen. Because of this, amine/amine exchange is thermodynamically governed by the basicity of the entering amine and a LFER does exist between basicity and aurophilicity. The experimental data are supported by simulations using a flat Au(111) surface as a model.

The total percentage of exchanged amines appears to depend on steric factors as secondary and tertiary amines replace a lower number of bound ones than primary amines do. Steric factors affect the strength of binding, too. The kinetic of the exchange process is bimodal with a fast process accounting for the first 63% of exchangeable amine ($t_{1/2}$ ranging from 15 to 46 s) and a slow one ($t_{1/2}$ ranging from 760 to 1824 s) accounting for the remaining 37%. These two processes constitute the first two steps in the cartoon representation of Figure 8.

The rates of exchange do not depend on the concentration of the added, entering amine, suggesting a dissociative, S_N1-like, mechanism, consistent with a weak N–Au(0) interaction. The relative ratio of the fast/slow exchange processes is the same for all amines (primary, secondary, and tertiary) and is likely related to the position, in the nanocrystal, of the Au(0) atom to which the

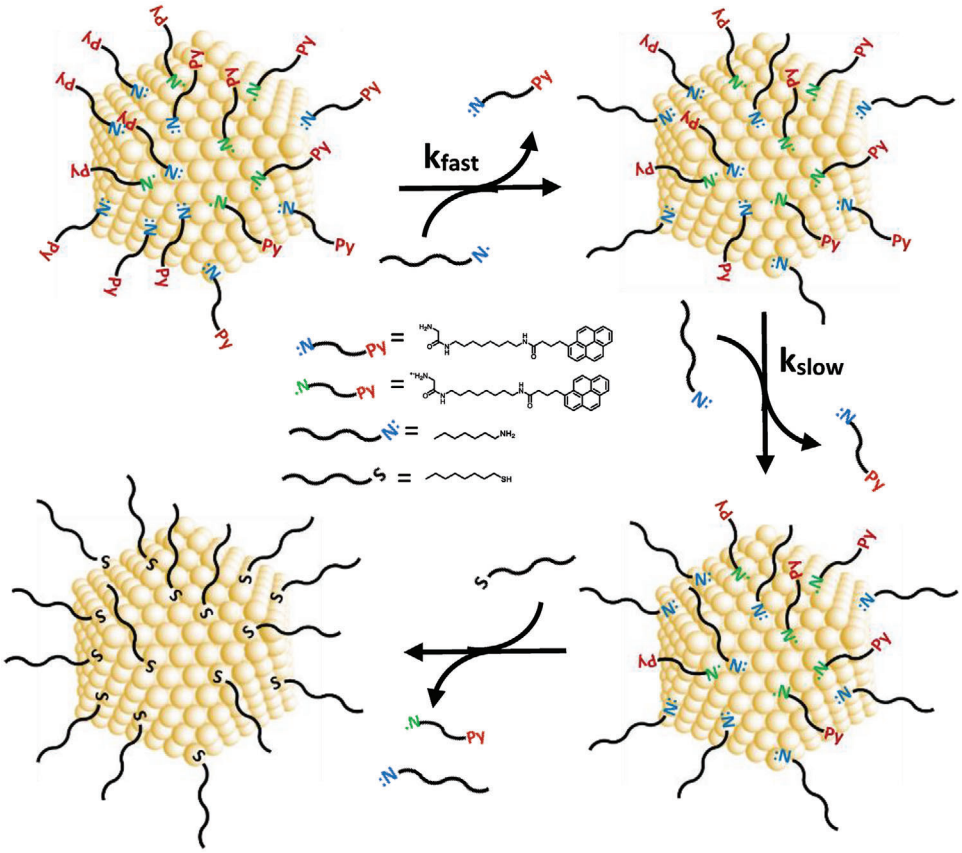

Figure 8. Cartoon representation of the amine exchange processes occurring on the gold nanoparticle surface (here arbitrarily presented as an icosahedron). The original passivation results in the formation of amines bound through their lone electron pair and those oxidized to form a radical cation (evolving to a radical after the loss of a proton). Upon addition of an entering amine, a first, fast exchange process occurs replacing the fluorescent amines bound to the flat surface with their lone electron pair, followed by a slower one replacing those on edges and vertexes with the same interaction. Removal of the amines interacting with the gold surface as radicals is only possible by adding a thiol (last step).

exiting amine is bound. We suggest that amines bound to flat (111) or (100) surfaces apparently exchange faster than those bound to lower coordination number gold atoms residing on rims and ridges. A stronger interaction with these atoms has been associated with their higher catalytic activity.[65]

However, these nanoparticles contain a sizeable amount of Au(I) on their surface (≈9% in our case). This allows the reduction of Au(I) present in the nanoparticles and the oxidation of the bound amines into radical cations that, after a loss of a proton, form Au(0)–RN/RN$^{\cdot+}$ bonds. Once this redox process has occurred it is impossible to replace the bound amine with an entering one, at least within the longest time scale we have followed our kinetics (≈72 h). Very likely the exchange process would become associative and only the addition of a thiol allows the complete removal of this fraction of amines to occur (third step in Figure 8). It is hence obvious that full exchange is only possible by using nanoparticles devoid of Au(I) atoms on their surface. The occurrence of such a redox process could play a role in the formation of a strongly bound protein corona when gold nanoparticles containing a fraction of Au(I) atoms are exposed to proteins with amino groups on their surface. Furthermore, AuNPs prepared using amines as reducing and passivating agents should be more stable than those obtained by passivation with an amine after the complete reduction process has occurred (by using a different reductant, for instance). This could be quite useful in preparing robust, protein-based nanozymes for biological applications where avoiding the exchange with serum proteins is an important requisite.

For technical reasons, the solvent of our investigation was ethanol and not water, the biological solvent. However, we believe that our conclusions can be extended to an aqueous environment in view of the existing correlation between the amine's pKa in the two solvents. The higher affinity of amines for protons than for Au atoms on nanoparticle surface implies that the pH constitutes a critical issue in controlling what drives the interaction of residues present on the surface of proteins with the bare surface of gold nanoparticles. Under conditions in which amino groups are not protonated we believe their pK_a could provide significant selectivity in binding. The matter is complicated by the fact that both the protein and the nanoparticle surface are multivalent and, hence, multiple interactions occur simultaneously with possible cooperative effects. By using proteins of similar valency, more basic ones will bind more strongly. With shorter peptides it appears evident that along with N-Au interactions also hydrophobic ones play a relevant role.[78,79] In ethanol hydrophobic interactions are less relevant. It also affects the secondary structure of proteins.

4. Experimental Section

The following experimental details are reported in the Supporting Information: general procedures; instrumentation used in the experiments performed throughout the paper; synthesis and characterization of the gold nanoparticles (TEM pictures, thermal gravimetric analysis, and surface coverage); surface exchange experiments and dissociation constants determination; exchange kinetics; study of the morphology of the nanoparticles by HRTEM; synthesis and characterization of the fluorescent probes (NMR spectra and ESI-MS data); computational methods used in studying the interaction of amines with the gold surface; voltammograms and electrochemical studies.

Supporting Information

Supporting Information is available from the Wiley Online Library or from the author.

Acknowledgements

Y.L., L.M.B., P.S., and F.M. thank the EU, Marie Curie program MSCA-ITN-2016, project MMBio (grant 721613) for financial support. Y.L. acknowledges the support by the China Scholarship Council for a fellowship.

Open Access Funding provided by Universita degli Studi di Padova within the CRUI-CARE Agreement.

Conflict of Interest

The authors declare no conflict of interest.

Author Contributions

Y.L. prepared the fluorescent probes and did all exchange experiments in collaboration with L.M.B. M.V. and S.C. are responsible of the computational analyses. M.C. and G.G. are responsible of the XPS experiments and their analysis. HRTEM images were collected and analyzed by P.R., P.B., and R.C. M.F. is responsible of the electrochemical studies. F.M. and P.S. conceived the study. All authors contributed to analyze the data and writing the manuscript.

Data Availability Statement

The data that support the findings of this study are available from the corresponding author upon reasonable request.

Keywords

amines, binding constants, gold nanoparticles, passivation

Received: December 12, 2022
Revised: February 27, 2023
Published online: April 28, 2023

[1] Y. Lyu, P. Scrimin, *ACS Catal.* **2021**, *11*, 11501.
[2] J. Czescik, S. Zamolo, T. Darbre, R. Rigo, C. Sissi, A. Pecina, L. Riccardi, M. D. Vivo, F. Mancin, P. Scrimin, *Angew. Chem., Int. Ed.* **2021**, *60*, 1423.
[3] X. Zhang, S. Lin, S. Liu, X. Tan, Y. Dai, F. Xia, *Coordin. Chem. Rev.* **2020**, *429*, 213652.
[4] L. Gabrielli, L. J. Prins, F. Rastrelli, F. Mancin, P. Scrimin, *Eur. J. Org. Chem.* **2020**, *2020*, 5044.
[5] J. Wu, X. Wang, Q. Wang, Z. Lou, S. Li, Y. Zhu, L. Qin, H. Wei, *Chem. Soc. Rev.* **2019**, *48*, 1004.
[6] D. Jiang, D. Ni, Z. T. Rosenkrans, P. Huang, X. Yan, W. Cai, *Chem. Soc. Rev.* **2019**, *48*, 3683.
[7] M. Liang, X. Yan, *Acc. Chem. Res.* **2019**, *52*, 2190.
[8] Y. Huang, J. Ren, X. Qu, *Chem. Rev.* **2019**, *119*, 4357.
[9] L. Qin, G. Zeng, C. Lai, D. Huang, P. Xu, C. Zhang, M. Cheng, X. Liu, S. Liu, B. Li, H. Yi, *Coord. Chem. Rev.* **2018**, *359*, 1.
[10] J. Wang, A. J. Drelich, C. M. Hopkins, S. Mecozzi, L. Li, G. Kwon, S. Hong, *Wiley Interdiscip. Rev. Nanomed. Nanobiotechnol.* **2021**, *14*, e1754.
[11] P. Zhang, J. Yang, D. Liu, *Electrophoresis* **2019**, *40*, 2211.
[12] X. Yang, M. Yang, B. Pang, M. Vara, Y. Xia, *Chem. Rev.* **2015**, *115*, 10410.
[13] W. Zhou, X. Gao, D. Liu, X. Chen, *Chem. Rev.* **2015**, *115*, 10575.
[14] T. Kang, Y. G. Kim, D. Kim, T. Hyeon, *Coordin. Chem. Rev.* **2020**, *403*, 213092.
[15] H. Kang, J. T. Buchman, R. S. Rodriguez, H. L. Ring, J. He, K. C. Bantz, C. L. Haynes, *Chem. Rev.* **2018**, *119*, 664.
[16] W. Kurashige, Y. Niihori, S. Sharma, Y. Negishi, *Coordin. Chem. Rev.* **2016**, *320*, 238.
[17] E. Pensa, E. Cortés, G. Corthey, P. Carro, C. Vericat, M. H. Fonticelli, G. Benítez, A. A. Rubert, R. C. Salvarezza, *Acc. Chem. Res.* **2012**, *45*, 1183.
[18] E. Pensa, L. M. Azofra, R. C. Salvarezza, P. Carro, *J. Phys. Chem. Lett.* **2022**, *13*, 6475.
[19] H. Al-Johani, E. Abou-Hamad, A. Jedidi, C. M. Widdifield, J. Viger-Gravel, S. S. Sangaru, D. Gajan, D. H. Anjum, S. Ould-Chikh, M. N. Hedhili, A. Gurinov, M. J. Kelly, M. E. Eter, L. Cavallo, L. Emsley, J.-M. Basset, *Nat. Chem.* **2017**, *9*, 890.
[20] D.-B. Grys, B. de Nijs, A. R. Salmon, J. Huang, W. Wang, W.-H. Chen, O. A. Scherman, J. J. Baumberg, *ACS Nano* **2020**, *14*, 8689.
[21] M. Bajaj, N. Wangoo, D. V. S. Jain, R. K. Sharma, *Sci. Rep.* **2020**, *10*, 8213.
[22] D. V. Leff, L. Brandt, J. R. Heath, *Langmuir* **1996**, *12*, 4723.
[23] S. Gomez, K. Philippot, V. Collière, B. Chaudret, F. Senocq, P. Lecante, *Chem. Comm.* **2000**, *2000*, 1945.
[24] M. Aslam, L. Fu, M. Su, K. Vijayamohanan, V. P. Dravid, *J. Mat. Chem.* **2004**, *14*, 1795.
[25] F. Manea, C. Bindoli, S. Polizzi, L. Lay, P. Scrimin, *Langmuir* **2008**, *24*, 4120.
[26] X. Lu, H. Tuan, B. A. Korgel, Y. Xia, *Chem. Eur. J.* **2008**, *14*, 1584.
[27] E. Yildirim, R. K. Ramamoorthy, R. Parmar, P. Roblin, J. A. Vargas, V. Petkov, A. Diaz, S. Checchia, I. R. Ruiz, S. Teychené, L.-M. Lacroix, G. Viau, *J. Phys. Chem. C* **2023**, *127*, 3047.
[28] D. I. Gittins, F. Caruso, *Angew. Chem., Int. Ed.* **2001**, *40*, 3001.
[29] Y. Imura, C. Morita, H. Endo, T. Kondo, T. Kawai, *Chem. Comm.* **2010**, *46*, 9206.
[30] Olmos-Asar, M. Ludueña, M. Mariscal, *Phys. Chem. Chem. Phys.* **2014**, *16*, 15979.
[31] Z. E. Hughes, T. R. Walsh, *Phys. Chem. Chem. Phys.* **2016**, *18*, 17525.
[32] L. B. Wright, P. M. Rodger, S. Corni, T. R. Walsh, *J. Chem. Theory. Comput.* **2013**, *9*, 1616.
[33] B.-K. Pong, J.-Y. Lee, B. L. Trout, *Langmuir* **2005**, *21*, 11599.
[34] R. C. Hoft, M. J. Ford, A. M. McDonagh, M. B. Cortie, *J. Phys. Chem. C* **2007**, *111*, 13886.
[35] D. Docter, D. Westmeier, M. Markiewicz, S. Stolte, S. K. Knauer, R. H. Stauber, *Chem. Soc. Rev.* **2015**, *44*, 6094.
[36] T. A. Papafilippou, M. Hadjidemetriou, in *World Scientific Series in Nanoscience and Nanotechnology*, World Scientific Publishing Co., Singapore **2022**, pp. 73–99.

[37] Y. Liu, Y. Xiang, D. Ding, R. Guo, *RSC Adv.* **2016**, *6*, 112435.
[38] C. Liu, T. Wu, Y. Lin, C. Liu, S. Wang, S. Lin, *Small* **2016**, *12*, 4127.
[39] L. Zuo, M. A. Hossain, B. Pokhrel, W.-S. Chang, H. Shen, *Adv. Sens. Energy Mater.* **2022**, *1*, 100024.
[40] J. Lou-Franco, B. Das, C. Elliott, C. Cao, *Nano-Micro Lett.* **2021**, *13*, 10.
[41] M. Wuithschick, A. Birnbaum, S. Witte, M. Sztucki, U. Vainio, N. Pinna, K. Rademann, F. Emmerling, R. Kraehnert, J. Polte, *ACS Nano* **2015**, *9*, 7052.
[42] H. Hinterwirth, S. Kappel, T. Waitz, T. Prohaska, W. Lindner, M. Lämmerhofer, *ACS Nano* **2013**, *7*, 1129.
[43] J.-W. Park, J. S. Shumaker-Parry, *ACS Nano* **2015**, *9*, 1665.
[44] V. E. Bel'skii, L. A. Kudryavtseva, K. A. Derstuganova, A. B. Teitel'baum, B. E. Ivanov, *Bull. Acad. Sci. Ussr Div. Chem. Sci.* **1981**, *30*, 736.
[45] X. Han, J. Goebl, Z. Lu, Y. Yin, *Langmuir* **2011**, *27*, 5282.
[46] M. E. Leunissen, C. G. Christova, A.-P. Hynninen, C. P. Royall, A. I. Campbell, A. Imhof, M. Dijkstra, R. van Roij, A. van Blaaderen, *Nature* **2005**, *437*, 235.
[47] U. S. Raikar, V. B. Tangod, B. M. Mastiholi, V. J. Fulari, *Opt. Commun.* **2011**, *284*, 4761.
[48] B. I. Ipe, K. G. Thomas, S. Barazzouk, S. Hotchandani, P. V. Kamat, *J. Phys. Chem. B* **2002**, *106*, 18.
[49] a) C. Pezzato, B. Lee, K. Severin, L. J. Prins, *Chem. Commun.* **2012**, *49*, 469; b) C. Pezzato, L. J. Prins, *Nat. Commun.* **2015**, *6*, 7790.
[50] Y. Lyu, G. Marafon, Á. Martínez, A. Moretto, P. Scrimin, *Chemistry Eur. J.* **2019**, *25*, 11758.
[51] A. E. Lanterna, E. A. Coronado, A. M. Granados, *J. Phys. Chem. C* **2012**, *116*, 6520.
[52] E. de la Llave, R. Clarenc, D. J. Schiffrin, F. J. Williams, *J. Phys. Chem. C* **2014**, *118*, 468.
[53] M. Montalti, L. Prodi, N. Zaccheroni, G. Battistini, *Langmuir* **2004**, *20*, 7884.
[54] G. Battistini, P. G. Cozzi, J.-P. Jalkanen, M. Montalti, L. Prodi, N. Zaccheroni, F. Zerbetto, *ACS Nano* **2007**, *2*, 77.
[55] E. A. Meyer, R. K. Castellano, F. Diederich, *Angew. Chem., Int. Ed.* **2003**, *42*, 1210.
[56] B. Pinter, T. Fievez, F. M. Bickelhaupt, P. Geerlings, F. D. Proft, *Phys. Chem. Chem. Phys.* **2012**, *14*, 9846.
[57] X. Deng, Y. Han, L.-C. Lin, W. S. W. Ho, *Sep. Purif. Technol.* **2022**, *299*, 121601.
[58] J. A. MacPhee, A. Panaye, J.-E. Dubois, *Tetrahedron* **1978**, *34*, 3553.
[59] A. Panaye, J. A. MacPhee, J.-E. Dubois, *Tetrahedron* **1980**, *36*, 759.
[60] H. Irving, H. Rossotti, K. Taugbøl, H. Theorell, B. Thorell, *Acta Chem. Scand.* **1956**, *10*, 72.
[61] Y. B. Atalay, D. M. D. Toro, R. F. Carbonaro, *Geochim. Cosmochim. Ac.* **2013**, *122*, 464.
[62] T. A. Hamlin, B. van Beek, L. P. Wolters, F. M. Bickelhaupt, *Chem. Eur. J.* **2018**, *24*, 5927.
[63] M. Morgenthaler, E. Schweizer, A. Hoffmann-Röder, F. Benini, R. E. Martin, G. Jaeschke, B. Wagner, H. Fischer, S. Bendels, D. Zimmerli, J. Schneider, F. Diederich, M. Kansy, K. Müller, *ChemMedChem* **2007**, *2*, 1100.
[64] A. V. Myshlyavtsev, P. V. Stishenko, A. I. Svalova, *Phys. Chem. Chem. Phys.* **2017**, *19*, 17895.
[65] S. H. Brodersen, U. Grønbjerg, B. Hvolbæk, J. Schiøtz, *J. Catal.* **2011**, *284*, 34.
[66] M. Montalti, L. Prodi, N. Zaccheroni, R. Baxter, G. Teobaldi, F. Zerbetto, *Langmuir* **2003**, *19*, 5172.
[67] M. J. Hostetler, A. C. Templeton, R. W. Murray, *Langmuir* **1999**, *15*, 3782.
[68] C. L. Heinecke, T. W. Ni, S. Malola, V. Mäkinen, O. A. Wong, H. Häkkinen, C. J. Ackerson, *J. Am. Chem. Soc.* **2012**, *134*, 13316.
[69] Y. Wang, T. Bürgi, *Nanoscale Adv.* **2021**, *3*, 2710.
[70] H.-M. Gao, H. Liu, H.-J. Qian, G.-S. Jiao, Z.-Y. Lu, *Phys. Chem. Chem. Phys.* **2017**, *20*, 1381.
[71] T. Mondal, A. Sermiagin, D. Meyerstein, T. Zidki, H. Kornweitz, *Nanoscale* **2019**, *12*, 1657.
[72] B. R. Karimadom, H. Kornweitz, *Molecules* **2021**, *26*, 2968.
[73] I. Gallardo, J. Pinson, N. Vilà, *J. Phys. Chem. B* **2006**, *110*, 19521.
[74] A. Adenier, M. M. Chehimi, I. Gallardo, J. Pinson, N. Vilà, *Langmuir* **2004**, *20*, 8243.
[75] J. R. Reimers, M. J. Ford, A. Halder, J. Ulstrup, N. S. Hush, *Proc. Natl. Acad. Sci. U. S. A.* **2016**, *113*, E1424.
[76] X. Fenouillet, M. Benoit, N. Tarrat, *Adsorption* **2020**, *26*, 579.
[77] C. Cougnon, J. Mauzeroll, D. Bélanger, *Angew. Chem., Int. Ed.* **2009**, *48*, 7395.
[78] Z. E. Hughes, M. A. Nguyen, J. Wang, Y. Liu, M. T. Swihart, M. Poloczek, P. I. Frazier, M. R. Knecht, T. R. Walsh, *ACS Nano* **2021**, *15*, 18260.
[79] J. P. Palafox-Hernandez, Z. Tang, Z. E. Hughes, Y. Li, M. T. Swihart, P. N. Prasad, T. R. Walsh, M. R. Knecht, *Chem. Mater.* **2014**, *26*, 4960.